

# Characteristic of Unsaturated Soil of Earth Fill Dams in Vietnam

Nguyen Thi Ngoc Huong<sup>1</sup> and Trinh Minh Thu<sup>2</sup>

<sup>1,2</sup>Department of Geotechnical Engineering, Thuyloi University, Hanoi, Vietnam

E-mail: tmthu@tlu.edu.vn

**ABSTRACT:** In Vietnam, earth dams are generally used with in-situ soils having low clay content (especially earth dams at the central part of Vietnam). The knowledge, experience, theory for calculation, apparatus for unsaturated soils in Vietnam are still very limited, especially the studies of the influences of the shear strength of unsaturated soils to the stability of earthen structures. Therefore, the research to study the soil-water characteristic curve, shear strength and coefficient of permeability versus different matric suction on Vietnamese soil is an urgent issue and it has big scientific and practical meaning. This research shows that when the matric suction in the soil changes, the effective cohesion  $c'$  would change, however the internal friction angle,  $\phi'$ , is almost unchanged for some type of soil in Vietnam. The experimental results would be applied to study the affect of unsaturated soil to the factor of safety of the slope.

**KEYWORDS:** Unsaturated soils, Earth fill dam, Seepage, Slope stability, Shear strength, Soil-water characteristic

## 1. INTRODUCTION

Large scale slope incidents in the world and in Vietnam were mostly related to the unsaturated state of soil. Instability problems often happen in earthen slopes that are formed by residual soils with deep ground water table.

It is possible to assume that the negative pore water pressure can be neglected for cases that larger part of the slip surface is located under the water level. However, in the situation that the ground water level is deep or when the shallow failure is predicted to happen, it would be not reasonable to ignore the negative pore water pressure.

The matric suction, soil water characteristic curve, permeability coefficient and shear strength are basic parameters of unsaturated soil. The shear strength of unsaturated soil is different from saturated soil by the cohesion due to matric suction. This additional cohesion depends on  $(u_a - u_w)$ , and the value of  $\phi^b$ .

The theory about unsaturated soil mechanics was established from many decades ago. Until now, we have had a quite stable background about the theory of unsaturated soil mechanics. Terzaghi (1936) used the Mohr – Coulomb criteria and the definition about effective stress to describe the shear strength of saturated soil. To determine the stress state for unsaturated soil, more and more researches have accepted the using of two independent stress state variables (Fredlund and Morgenstern, 1977).

In Vietnam, problems related to unsaturated soil mechanics was just started to study in recent years. A few publications and researches about unsaturated soil has been announced, the theory of unsaturated soil mechanics related to permeability, stability, stress - strain has been applied to calculate the stability of structures. Especially, the geotechnical engineering laboratory - Water Resources University has had an equipment to define the soil water characteristic (SWCC) and the shear strength of unsaturated soil, contributing to experimental research for defining unsaturated soil parameters in Vietnam.

The problem to study and apply laboratory equipment, laboratory procedures to determine unsaturated soil parameters and apply these parameters in calculating the stability of earth structures in Vietnam have a great meaning and necessary, it starts a new research direction for Vietnamese scientists. Together with the world's scientists we also have a great contribution on the development and fulfillment the theory in unsaturated soil mechanics. In this research, the author suggests a study to define unsaturated soil parameters for some soil types in Vietnam and apply these parameters in earth dam stability calculation.

## 2. THEORETICAL BASIS OF UNSATURATED SOIL

### 2.1 Stress state variables in soil

Bishop (1959) suggested an experimental equation to define the effective stress and it has been applied popularly (for example the lecture in Oslo, Norway, 1955):

$$\sigma' = (\sigma - u_a) + \chi(u_a - u_w) \quad (1)$$

where:  $u_a$  – pore air pressure;  $\chi$  - the parameter related to the degree of situation.

In 1977, Fredlund and Morgenstern has studied and concluded that any two of three normal stress variables (total stress  $\sigma$ , pore water pressure  $u_w$  and pore air pressure  $u_a$ ) can be used to describe the stress state of unsaturated soil. In other words, three combinations can be used to describe stress state variables, compatible with soil structure and the surface tension in unsaturated soil:  $(\sigma - u_a)$  and  $(u_a - u_w)$ ;  $(\sigma - u_w)$  and  $(u_a - u_w)$ ;  $(\sigma - u_a)$  and  $(\sigma - u_w)$ , where:  $\sigma$  - total stress;  $u_a$  – pore air pressure;  $u_w$  – pore water pressure.

### 2.2 The soil water characteristics

In unsaturated soil mechanics, the relation curve between the soil moisture versus matric suction is defined as the soil water characteristic. It has a great meaning in solving seepage problems in unsaturated soil mechanics, controlling parameters of unsaturated soil such as the permeability coefficient, shear strength and volumetric strain of soil.

Many types of experimental equations have been proposed to perform the soil water characteristic curve. The equation form that is used to illustrate the relationship between the matric suction and moisture content is the equation of Fredlund & Xing (1994).

Fredlund and Xing:

$$\Theta = C(\psi) \left\{ \frac{1}{\ln \left[ e + \left( \frac{\psi}{a} \right)^n \right] \right\}}^m \quad (2)$$

where:  $\alpha$ ,  $a$ ,  $n$ ,  $m$  – constants (different parameters of soil),  $\psi$  - matric suction,  $\Theta$  - volumetric water content,  $\Theta = (\theta - \theta_r) / (\theta_s - \theta_r)$  ( $\theta_s$  is the volumetric water content at saturation,  $\theta_r$  is the residual volumetric water content, and  $\theta$  is the volumetric water

content at a specific matric suction),  $e$  - the log base number, and  $C(\psi)$  - the adjusted coefficient.

**2.3 The shear strength of unsaturated soil**

**2.3.1 The saturated soil shear strength equation**

Terzaghi (1936) used the Mohr – Coulomb criteria and the effective stress definition to describe saturated soil shear strength:

$$\tau_{ff} = c' + (\sigma_f - u_w)_f \tan \phi' \tag{3}$$

where:  $\tau_{ff}$  – shear stress on the failure plane at failure;  $c'$  – the effective cohesion;  $(\sigma_f - u_w)_f$  – the effective normal stress on the failure plane at failure;  $\phi'$  – the effective internal friction angle.

**2.3.2 The shear strength equation of unsaturated soil**

Bishop (1959) proposed a shear strength equation as follow:

$$\tau = c' + [(\sigma - u_a) + \chi(u_a - u_w)] \tan \phi' \tag{4}$$

where:  $c'$  - the effective cohesion;  $\phi'$  - the effective internal friction angle of saturated soil,  $\sigma$  - the total normal stress,  $u_a$  - pore air pressure, and  $\chi$  - a parameter related to the soil degree of saturation, vary from 0 to 1.

Fredlund et al. (1978) suggested a shear strength equation for unsaturated soil by using stress state variables  $(\sigma - u_a)$  and  $(u_a - u_w)$  as follow:

$$\tau_{ff} = c' + (\sigma_f - u_a)_f \tan \phi' + (u_a - u_w)_f \tan \phi^b \tag{5}$$

where:  $\tau_{ff}$  – the shear stress on the failure surface at failure state,  $c'$  - effective cohesion,  $(\sigma_f - u_a)_f$  – net normal stress on the failure surface at failure state,  $\phi'$  – effective internal friction angle corresponding to the net normal stress  $(\sigma_f - u_a)_f$ ,  $(u_a - u_w)_f$  – matric suction at failure state, and  $\phi^b$  – the angle that shows the velocity of the increase in shear strength corresponding to the increase in the matric suction  $(u_a - u_w)_f$  at failure state.

Vanapalli et al. (1996) and Fredlund et al. (1996) suggested a function to predict the shear strength of unsaturated soil from the SWCC and effective shear strength parameters ( $c'$  and  $\phi'$ ) as follow:

$$\tau = c' + (\sigma_n - u_a) \tan \phi' + (u_a - u_w) \left[ \Theta^\kappa (\tan \phi') \right] \tag{6}$$

where:  $\kappa$  - a adjusted argument used to find the calculated values that fit the measured values;  $\Theta$  - the volumetric water content that has been normalized ( $\Theta = \theta_w / \theta_s$ );  $\theta_w$  – volumetric water content;  $\theta_s$  – volumetric water content at saturation

**2.4 The method to analyze the permeability in the saturated and unsaturated environment**

The soil permeability coefficient can be determined by indirect method from SWCC or direct method (the permeability test). Leong and Rahardjo (1977) suggested an equation to predict the permeability coefficient based on the saturated permeability coefficient and the soil water characteristic curve, as follow:

$$k_w = k_s \Theta^p = k_s \left( \frac{\theta_w}{\theta_s} \right)^p \tag{7}$$

where:  $p$  is a constant. Fredlund et al. (2011) has determined constant  $p$  for many pair of data and has found out the variation of  $p$  from 2, 4 to 5,6 for different soils. The average value of  $p$  for any type of soil is 3,29.

**3. EXPERIMENTAL RESEARCH FOR OBTAINING UNSATURATED SOIL PROPERTIES**

**3.1 Basis soil properties**

The research is concentrated to study on unsaturated soil at three areas in Vietnam: on the North – West, North - East and in the Central part. The compacted soils used for testing are at the Ninhthuan dam of Phuocthang village, Bacai Distric and Ninhthuan province. The second compacted soils for testing is at the Khecat earth fill dam of Hailang village, Tienyen district and Quangninh province. The third soils are undisturbed samples at the natural slope of Yenbai city, Yenbai province. The procedure of the soil testing was following Vietnam Standards (TCVN) 1995 and soil properties are presented in Table 1.

Table 1 Soil properties of the compacted specimens

Soil properties	Notation	Unit	Songsat 1	Songsat 2	Songsat 3	Khecat
Particle size						
>10.000 mm		%	0,00	0,21	2,59	0,00
5,000 - 10,000 mm		%	0,00	2,08	2,41	0,00
Gravel		%	0,00	4,89	6,25	9,00
2,000 - 5,000 mm		%	0,00	11,19	10,30	7,00
Sand		%	0,00	15,34	5,80	5,54
0,250 - 0,500 mm		%	15,11	9,69	10,30	13,00
0,100 - 0,250 mm		%	33,28	30,17	29,69	8,00
0,050 - 0,100 mm		%	12,22	9,68	8,93	15,00
Silt		%	0,97	1,29	1,22	11,00
0,010 - 0,050 mm		%	23,07	25,00	22,78	31,00
Clay		%				
<0,005 mm		%				
Specific Gravity	$G_s$		2,680	2,725	2,731	2,710
Liquid limit	$W_l$	%	24,83	23,83	24,08	52,60
Plastic limit	$W_p$	%	14,99	13,20	15,16	34,47
Plastic index	$I_p$	%	9,84	10,62	8,91	18,13
Maximum dry density	$\rho_{dmax}$	g/cm <sup>3</sup>	1,867	2,024	1,997	1,550
Optimum water content	$W_{opt}$	%	12,73	11,06	10,97	24,50

**3.2 Tests for obtaining soil-water characteristic curve (SWCC)**

**3.2.1 Apparatus for the Soil-water Characteristic Curve**

**Tests**

The pressure plate was used for obtaining the SWCC. Figure 1 shows the setup of the pressure plate with a 5 bar high air-entry ceramic disk and a rubber membrane beneath the disk.

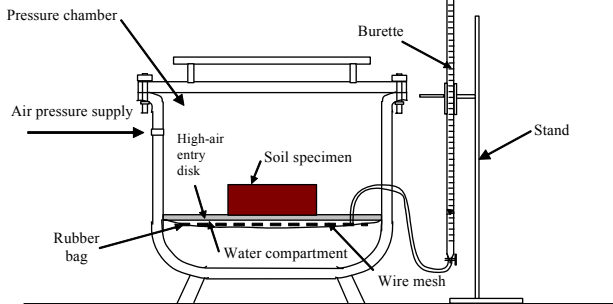


Figure 1 Pressure plate for obtaining SWCC

**3.2.2 Soil specimen preparation**

The statically compacted soil specimens used were 20 mm in thickness, 62 mm in diameter and volume of 60 cm<sup>3</sup>. The dry density was compacted at 95% of the maximum dry density and optimum water content. The soil samples at Yenbai were trimmed with 20 mm in thickness and volume of 60 cm<sup>3</sup>.

The specimens used for obtaining SWCC were prepared in the same manner as the soil specimens for triaxial tests. The space between the disk and the rubber membrane serves as a water compartment. The water compartment is connected to a burette line that is opened to atmospheric pressure. The number of specimens that can be tested in a pressure plate depends on the available disk space. The ceramic disk was saturated prior to test.

**3.2.3 Saturation soil specimen and pressure plate**

The saturation was done by pouring the de-aired distilled water on top of the disk and applying a high air pressure of 500 kPa while opening the valve of the burette line for about 1 hour. Due to the high pressure in the chamber, the distilled de-aired water infiltrated through the ceramic plate. The soil properties are presented in Table 2.

Table 2 Soil properties of the compacted specimen

Properties	Notation	Unit	Songsat 1	Songsat 2	Songsat 3	Khecat
Water content	$W_{cb}$	%	12,73	11,06	10,97	24,50
Wet unit weight	$\rho_{cb}$	g/cm <sup>3</sup>	2,000	2,136	2,105	1,830
Dry unit weight	$\rho_{deb}$	g/cm <sup>3</sup>	1,774	1,923	1,897	1,470
Volumetric water content	$\theta_s$		0,348	0,345	0,390	0,456
Coefficient of permeability at saturated condition	$k_s$	m/s	$5,0 \cdot 10^{-8}$	$1,6 \cdot 10^{-7}$	$2,0 \cdot 10^{-7}$	$1,9 \cdot 10^{-8}$

**3.2.4 Tests for obtaining SWCC**

In this test, the air pressure was applied at different level. The pore-air pressure,  $u_a$  was applied by air pressure, while water pressure opened to atmospheric pressure (i.e.,  $u_w = 0$  kPa and  $u_w = 0$  kPa), therefore the matric suction changing due to the change in applying air pressure. The tests for obtaining SWCC

were done with the matric suction of 10kPa, 20 kPa, 50 kPa, 100 kPa, 200 kPa and 400 kPa.

**3.2.5 Test results**

Figures 2 and 3 show the SWCC of 9 soil specimens. As indicated in the Figure 2, there was a significant decrease in volumetric water content when the matric suction in the specimen exceeded the air-entry value. The soil-water characteristic curve of the specimen indicated that the air-entry value (AEV) of the Khecat compacted soil specimen was 40 kPa. The air-entry values of the Songsat compacted soil specimens 1, 2 and 3, were 20,04 kPa, 20,08 kPa and 11,8 kPa respectively. The air-entry values of the Yenbai undisturbed soil specimens 1, 2, 3, 4 and 5, were 31 kPa, 26 kPa, 21 kPa, 20,8 kPa and 22 kPa as shown in Figure 3. The results show that in general  $I_p$  rose with the increase of the air-entry value.

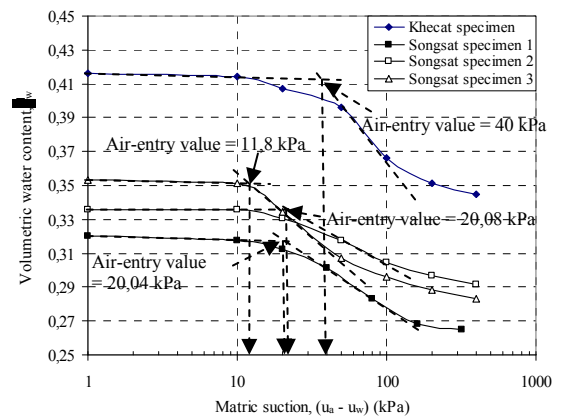


Figure 2 SWCC of Khecat and Songsat compacted soil specimens

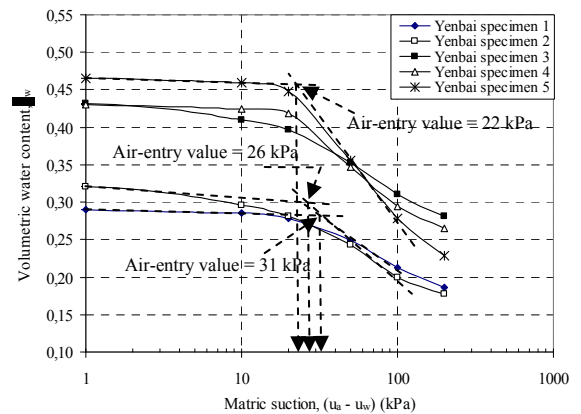


Figure 3 SWCC of the Yenbai undisturbed soil specimens

**3.2.6 Calculation coefficient of permeability from SWCC**

**• Calculation SWCC by using Fredlund and Xing (1994) method**

Equation of Fredlund and Xing (1994) has been widely used to determine SWCC. The details of the calculation SWCC by using method of Fredlund and Xing (1994) are presented in Figures from 4 to 7.

The figures show that the prediction results from equation of Fredlund and Xing (1994) are good agreement to the experimental results.

**• Prediction coefficient of permeability function from SWCC**

This study calculated coefficient of permeability at different volumetric water content by using Equation (7). The prediction of coefficient of permeability from SWCC by Fredlund and Xing (1994) for compacted soil specimens are presented in Figures 8, 9, 10 and 11.

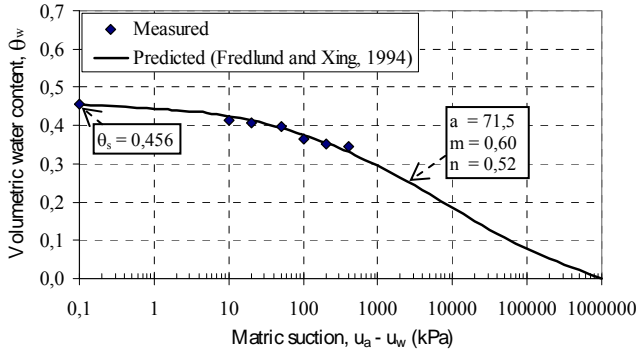


Figure 4 SWCC of the Khecat compacted soil

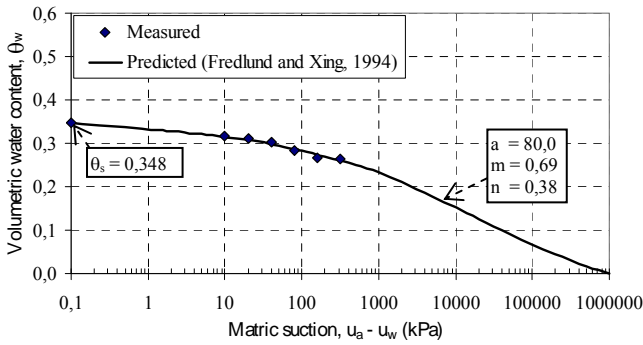


Figure 5 SWCC of the Songsat compacted soil specimen 1

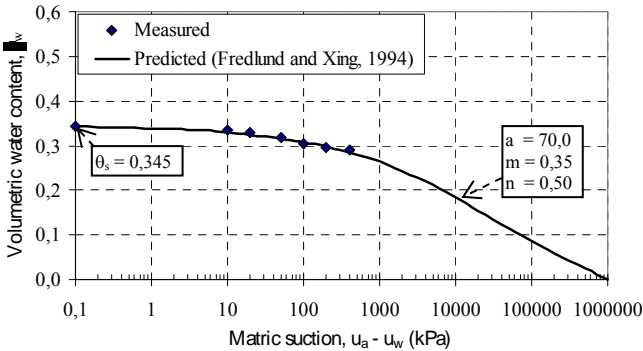


Figure 6 SWCC of the Songsat compacted soil specimen 2

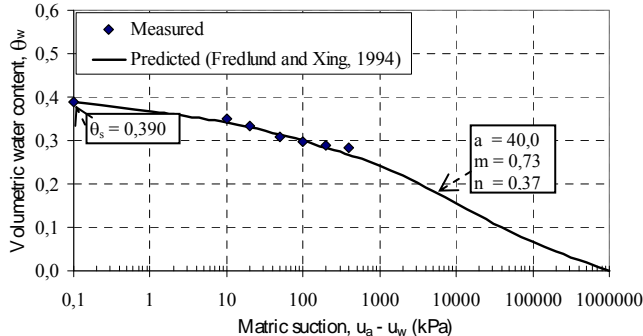


Figure 7 SWCC of the Songsat compacted soil specimen 3

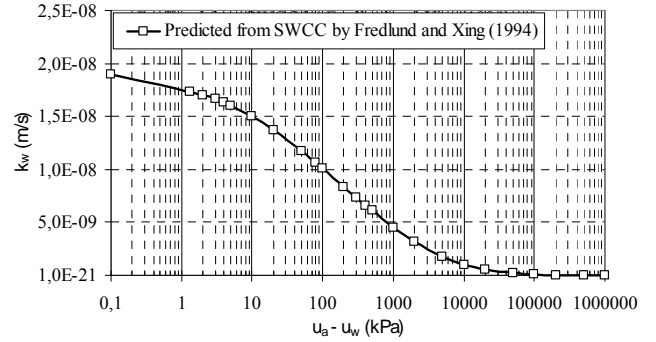


Figure 8 Coefficient of permeability versus matric suction of Khecat specimen

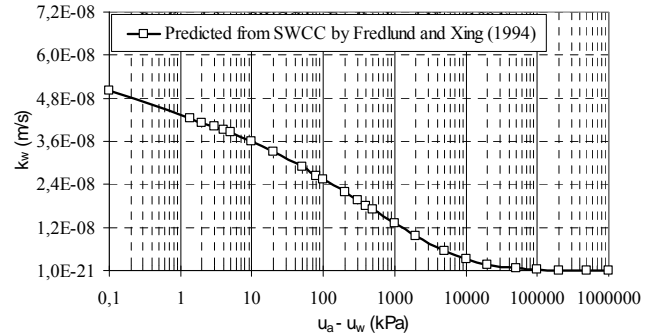


Figure 9 Coefficient of permeability versus matric suction of Songsat specimen 1

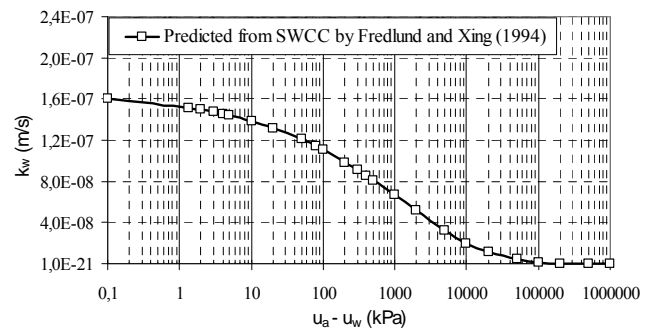


Figure 10 Coefficient of permeability versus matric suction of Songsat specimen 2

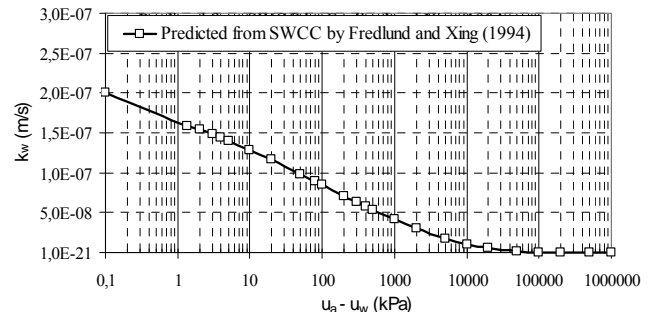


Figure 11 Coefficient of permeability versus matric suction of Songsat specimen 3

**3.3 Determination of shear strength for unsaturated soil by triaxial compression test**

**3.3.1 Modified triaxial compression apparatus for unsaturated soil test**

Modified triaxial compression apparatus used in this experiment is similar to Fredlund and Rahardjo one (1993) (Figure 12). The feature of this pressure cell is to replace the base porous disk by the high pressure ceramic one to control and measure the pore pressure of unsaturated soil. To control the pore air pressure during the consolidation and shear, the backpressure vane of the normal pressure cell becomes the control vane of air pore pressure (C). The high pressure disk in this research is the 5 bar (500 kPa) one.

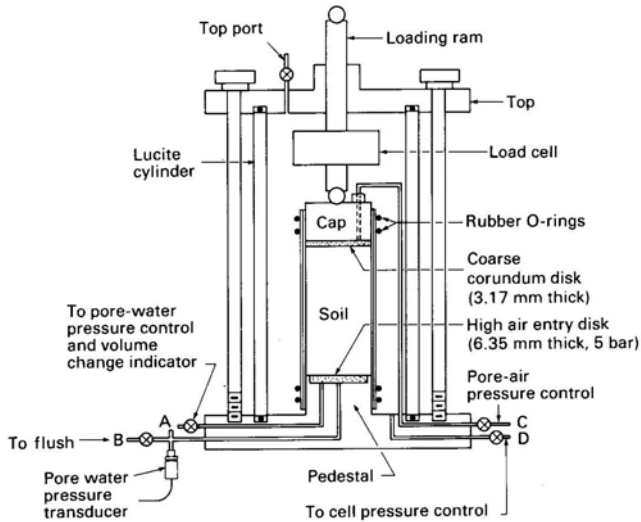


Figure 12 Modified triaxial cell for unsaturated soils testing (after Fredlund and Rahardjo, 1993)

### 3.3.2 Process and procedure of test

The triaxial compression test procedure for saturated soil sample (Head, 1986) and for unsaturated one (Fredlund and Rahardjo, 1993) have been used here. The initial matric suctions of the specimens were established using the axis-translation technique (Hilf, 1956).

#### • Soil sample preparation

The soil samples are compacted at dry unit mass equal 95% of maximum unit one with corresponding moisture content after compacting (Table 2). The height and diameter of the soil sample are respectively equal 100 mm and 50 mm.

#### • Saturation phase of soil sample

All of the samples used in this experiment programme are saturated first aiming at creating the identically initial moisture content. After that the samples are saturated by means of gradually increasing the confining pressure ( $\sigma_3$ ) and backpressures,  $u_w$ , under effective stress equal 10 kPa until the coefficient of water pore pressure B attains proximity of 1.

#### • Consolidation phase

After finishing saturation phase, the soil sample are consolidated under confined pressure,  $\sigma_3$ , and pore water pressure,  $u_w$ , or in other words it is isotropically consolidated under require effective stresses,  $(\sigma_3 - u_w)$ . The consolidation phase is considered to end when the water volume escaped from the soil sample unchanged and the excess pore pressure is completely dissipated. The time for consolidation phase is about 1 hour.

#### • Phase of creating and balancing the matric suction in soil sample

The matric suction balancing phase is to create the matric suction inside the soil sample when finishing the consolidation one. In the process of creating the matric suction, the soil sample will be consolidated by the real confined pressure ( $\sigma_3 - u_a$ ) and the matric suction ( $u_a - u_w$ ). This phase is considered to finish when the escaped water is quasi 0. The time for balancing the matric suction elongates about 3 to 5 days.

#### • The shearing phase of soil sample

When attaining the condition of balancing the matrix suction phase under applied pressures (i.e  $\sigma_3$ ,  $u_a$  and  $u_w$ ), the soil sample is sheared by axial pressure in conditions of air escape and no for pore water (schema CW) or both air and pore water escape (schema CD), with constant velocity of shearing. In this study, the displacement velocity of 0,02 mm/minute is selected. The procedure of shearing is finished at maximum deviatoric stress. If the above failure condition is not accessible, stop the experiment at 25% of axial deformation. The shearing phase elongates in 24 hours.

### 3.3.3 Test program

Triaxial compression test was using the compacted soil samples of Khecat and Songsat 3, in which 9 samples of Khecat (according to schema CD) and 18 samples of Songsat 3 (according to schema CD and CW).

### 3.3.4 The results of triaxial compression test using consolidated - Drained (CD) schema

#### • Experimental results of Khecat compacted samples

\* Shear strength properties of experimental soil samples

The Figures 13 and 14 show the relationship between deviator stresses and axial strains under different real confined pressure with the same matric suction equal 0 kPa and 200 kPa. At the same matric suction equal 0 kPa, the more the samples sustained higher net confining pressure, the more the peak deviator stress increases. At the same matric suction, when the real confined pressure gradually increases on the soil sample, its shear strength also increases correspondingly.

\* The extended Mohr-Coulomb failure envelope surface

The extended Mohr-Coulomb failure envelope surface is given in the Figure 15. On the Figure 15, it is shown that the envelope surface is curve along the matric suction axe. Projection of the failure envelope surface on the  $\tau \sim (\sigma - u_a)$  plane gives the matric suction contours as shown in the Figure 16. These lines have different cohesive intercepts belong to their correspondent matric suctions. The intercepts become effective cohesion  $c' = 37$  kPa when the matric suction tends to 0.

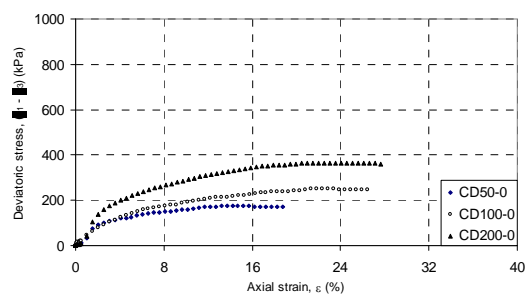


Figure 13  $(\sigma_1 - \sigma_3)$  versus  $\epsilon$  with the same initial matric suction of 0 kPa

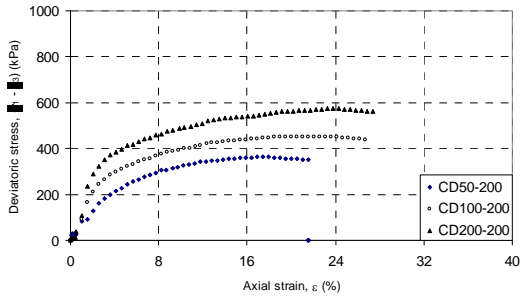


Figure 14 ( $\sigma_1 - \sigma_3$ ) versus  $\epsilon$  with the same initial matric suction of 200 kPa

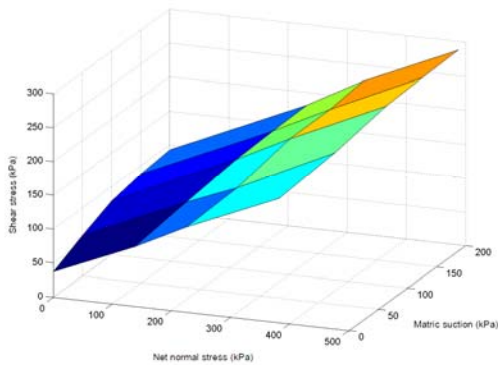


Figure 15 Extended Mohr-Coulomb failure envelope of Khecat specimen for CD tests

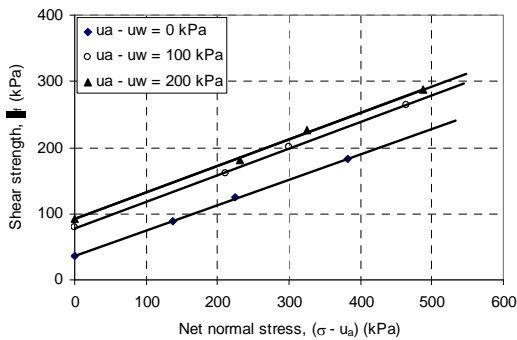


Figure 16 Horizontal projections of the failure envelope onto the  $\tau_f$  versus  $(\sigma - u_a)$  plane

All identical matric suction lines have the same slope angle  $\phi^b = 23^\circ$ . Projections of the failure envelope surfaces on the  $\tau \sim (u_a - u_w)$  plane are curve lines shown in the Figure 17. These projections show the increase of shear strength when the matric suction increases at each real normal stress.

The increasing law of the shear strength with matric suction is curvilinear. At the same matric suction, the more real confined pressure is great, the more shear strength increases.

• **Experimental results of Songsat 3 compacted samples**

\* Shear strength properties of experimental soil sample

The relationships between deviator stress and strain under different confined pressures at the same matric suction equal 0 kPa and 200 kPa are shown in the Figures 18 and 19. From Figure 18, it is shown that the peak deviator stress is influenced by the real confined pressure: the increase of confined pressure increases the peak deviator stress.

With the matric suction equal 200 kPa in the Figure 19, the shear strength is more increased in comparison with which equal 0 and 100 kPa. It shows that the matric suction increases the shear strength of the sample.

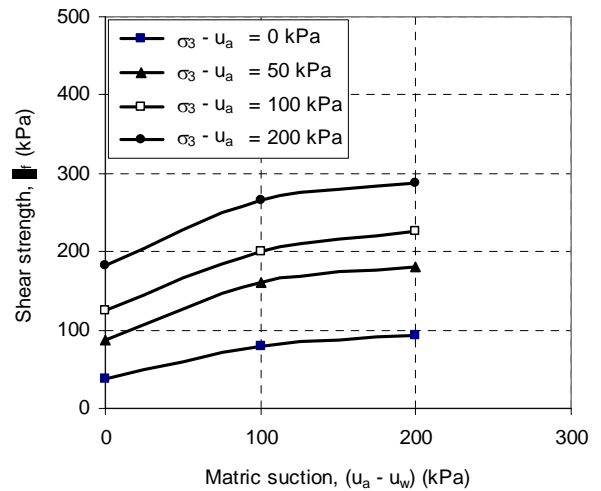


Figure 17 Horizontal projections of the failure envelope onto the  $\tau_f$  versus  $(u_a - u_w)$  plane

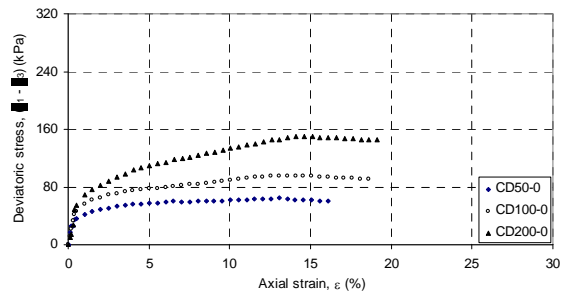


Figure 18 ( $\sigma_1 - \sigma_3$ ) versus  $\epsilon$  with the same initial matric suction of 0 kPa

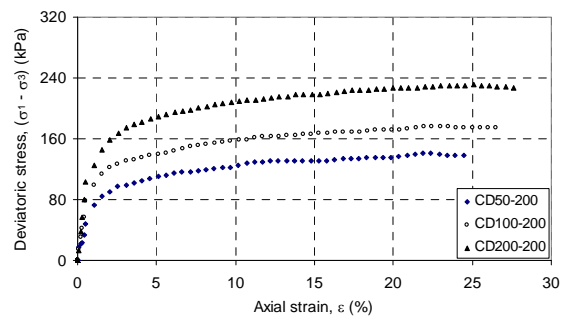


Figure 19 ( $\sigma_1 - \sigma_3$ ) versus  $\epsilon$  with the same initial matric suction of 200 kPa

\* The extended Mohr- Coulomb failure envelope surface

The extended Mohr-Coulomb failure envelope surface is shown in the Figure 20. Figure 20 shows the trend of decreasing  $\phi^b$  when increasing the matric suction however  $\phi^b$  nearly unchanged and  $\phi^b = \phi^a$  when the matric suction is less than the critical air entry value. Projections of the failure envelope surfaces on the  $\tau \sim (\sigma - u_a)$  plane give the matric suction contours as shown in the Figure 21. All identical matric suction lines have the same slope angle  $\phi^a = 13^\circ$ .

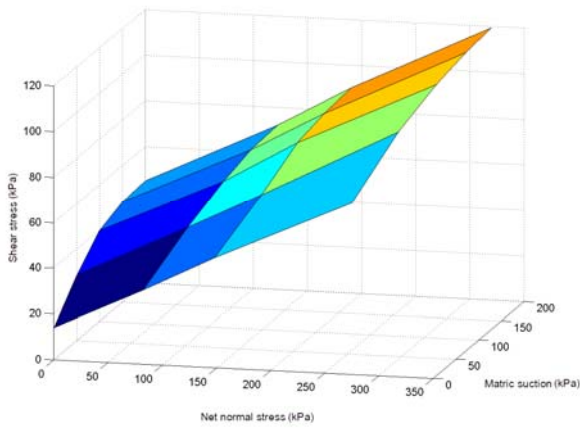


Figure 20 Extended Mohr-Coulomb failure envelope of Songsat specimen 3 for CD tests

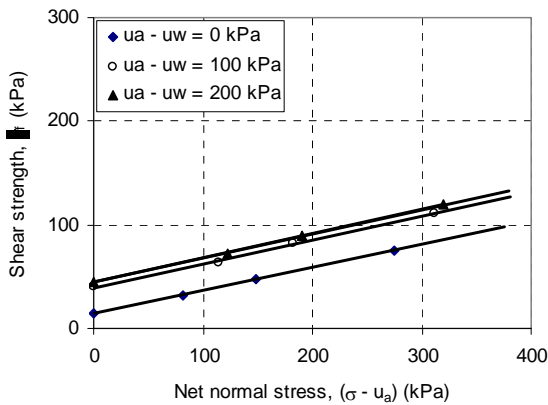


Figure 21 Horizontal projections of the failure envelope onto the  $\tau_f$  versus  $(\sigma - u_a)$  plane

Projections of the failure envelope surfaces on the  $\tau \sim (u_a - u_w)$  plane are shown by the curves in the Figure 22. The intersection lines show the increase of shear strength value when increasing the matric suction.

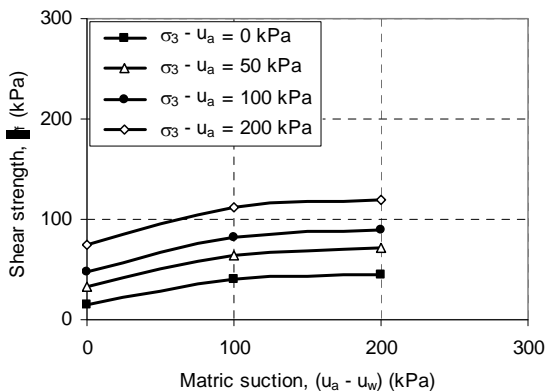


Figure 22 Horizontal projections of the failure envelope onto the  $\tau_f$  versus  $(u_a - u_w)$  plane

### 3.3.5 The results of triaxial compression test with unchanged moisture content (CW)

#### • Shear strength characteristics of experimental soil samples

The Figures 23 and 24 show the relationship between deviatoric stresses and axial strains under different real confined pressures (50 kPa, 100 kPa and 200 kPa) acting upon soil samples with each same matric suction equal 0 kPa and 200 kPa alternatively. This is shown that the more unsaturated condition of the sample the more increase of the shearing strength.

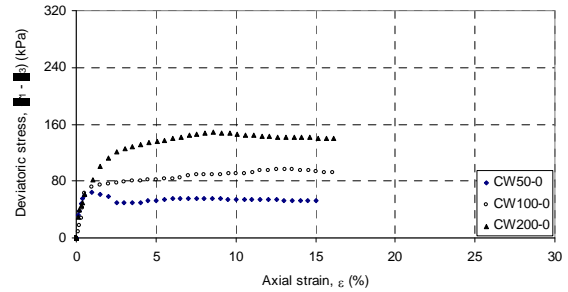


Figure 23  $(\sigma_1 - \sigma_3)$  versus  $\epsilon$  with the same initial matric suction of 0 kPa

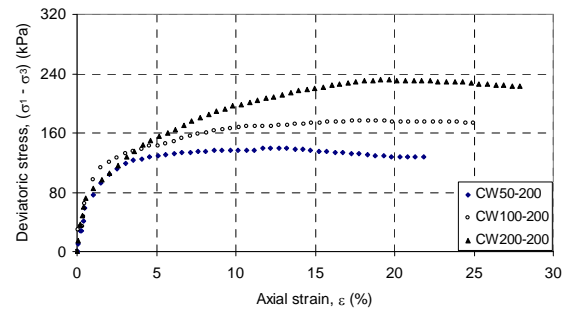


Figure 24  $(\sigma_1 - \sigma_3)$  versus  $\epsilon$  with the same initial matric suction of 200 kPa

#### • Excess pore pressure

The Figures 25 and 26 show the variation of pore water pressure during shear in triaxial test with constant water content (CW) on saturated soil samples under different real confined pressures at the same initial matric suction equal 0 kPa and 200 kPa respectively.

#### • The extended Mohr-Coulomb failure envelope surface

The extended Mohr-Coulomb failure envelope surface is shown in the Figure 27. From this figure, it is seen that: when increasing the matric suction,  $\phi^b$  is reduced from  $\phi^b = \phi'$  at the 0 kPa until  $\phi^b = 4^\circ$  in accordance with 200 kPa matric suction. The angle of internal friction  $\phi'$  of the soil sample seemed still to keep true to  $13^\circ$  despite the matric suction increases.

Projection of the failure envelope surface on the  $\tau \sim (\sigma - u_a)$  plane is shown in Figure 28. All of identical matric suction lines have the same slope angle  $\phi' = 13^\circ$ . Projection of the failure envelope surface on the  $\tau \sim (u_a - u_w)$  plane is shown in Figure 29. The intersection lines show the increase of shear strength when increasing the matric suction. The relationships in the Figure 29 show that the shear strength of the soil samples increase when the matric suction increase. The real confined pressures increase also make to increase the shear strength of the soil sample respectively.

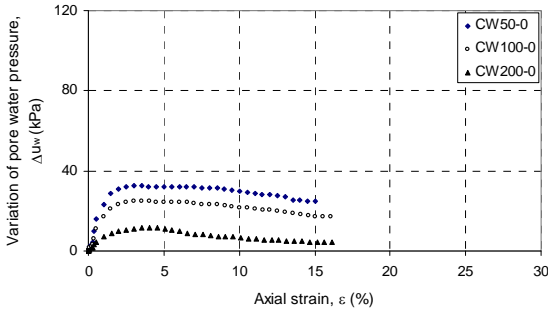


Figure 25  $u_w$  versus  $\epsilon$  with the same initial matric suction of 0 kPa

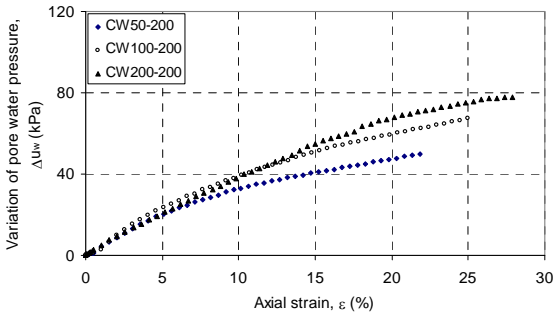


Figure 26  $u_w$  versus  $\epsilon$  with the same initial matric suction of 200 kPa.

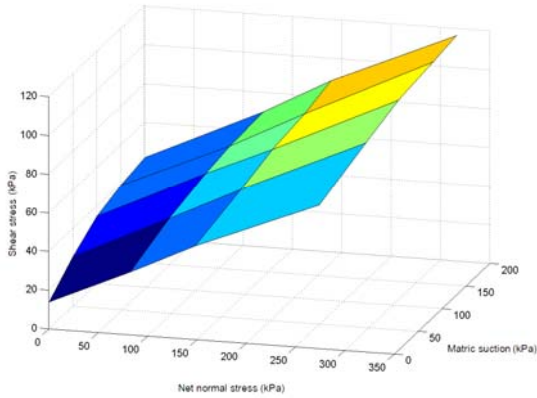


Figure 27 Extended Mohr-Coulomb failure envelope of SongSat specimen 3 for CW tests

**3.4 Analysis of test result**

The comparison of the shear strength versus matric suction curves of two triaxial compression tests carried out according to CD and CW methods for the SongSat 3 compacted soil samples shows that the CW curve fairly near the CD one.

Table 3 gives the effective parameters of the shear strength ( $\phi'$  and  $c'$ ) of test soil samples. As seen in the Table 3, the shear strength effective parameters ( $\phi'$  and  $c'$ ) of the same material done in different shear methods (direct shear, consolidated-drained and constant water content shear) give nearly the same. As also seen that when the matric suction equal 0,  $\phi^b \approx \phi'$  and when the matric suction increases until some value, the angle  $\phi^b$  gradually decreases.

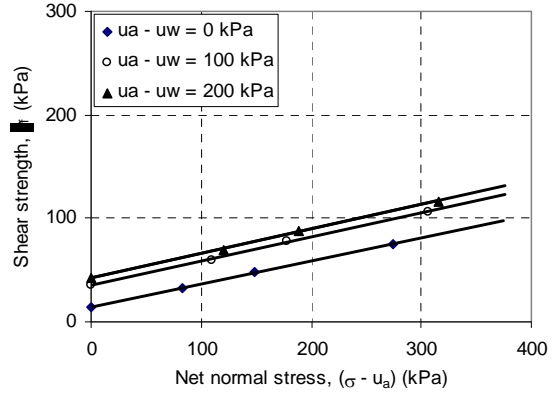


Figure 28 Horizontal projections of the failure envelope onto the  $\tau_f$  versus  $(\sigma - u_a)$  plane

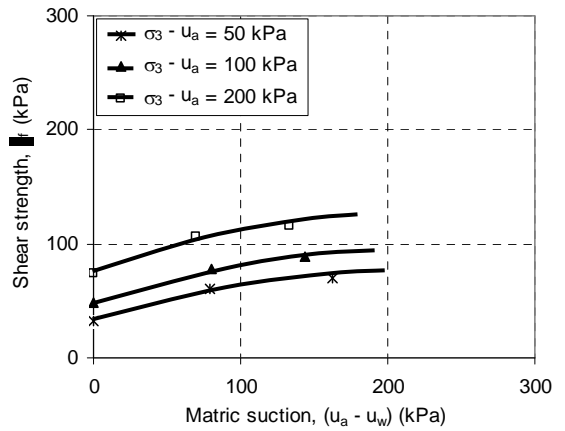


Figure 29 Horizontal projections of the failure envelope onto the  $\tau_f$  versus  $(u_a - u_w)$  plane

Table 3 Comparison of the effective parameters of shear strength

Effective parameters of shear strength	Khecat material quarry		Songsat 3 material quarry			
	Direct shear test	CD test	Direct shear test	CD test	CW test	
$\phi'$ (degree)	23°29'	23°11'	13°03'	13°02'	13°00'	
$c'$ (kPa)	34,00	37,00	13,53	14,20	14,00	
$\phi^b$ (degree)						
	0	23,47	23,18	13,15	13,11	13,08
	20	23,35		12,99		
Matric suction (kPa)	50	23,03		12,37		
	100	10,11	7,97	5,24	4,86	4,12
	200	8,35	6,28	4,40	4,01	3,60

#### 4. APPLICATION OF THE RESEARCH RESULTS FOR CALCULATING SOME OF SLOPES IN VIETNAM

##### 4.1 Stability analysis of the songsat earth dam slope

###### 4.1.1 Seepage analysis

The analysis result of the pore water pressure using SEEP/W (GEOSTUDIO 2004) is shown in the Figure 30. From this, it is seen that the maximum value of negative pore pressure in the area of dam core is inferior -140 kPa, while in its downstream incremental loading area it is under -200 kPa.

###### 4.1.2 Slope stability analysis

In order to study the influence of the matric suction to the stability of the embankment, the three following method is used:

- ✦ No consideration of  $\phi^b$ : this method is applied in case no consideration of the influence of the unsaturated soil area above the saturation line.
- ✦ Assumption  $\phi^b = 1/2 \phi'$ : applied in case no having test practical material of unsaturated soil.
- ✦ Total cohesion: in case to have enough test material parameters of unsaturated soil, the total cohesion method will be applied in order to exactly analysis the actual working of the earth dam.

###### • Stability analysis according to no consideration of $\phi^b$ method

The result of stability analysis for the downstream slope without consideration of  $\phi^b$  gives the minimum factor of stability equal 1,195 ( $F_s = 1,195$ ).

###### • Stability analysis according to the assumption $\phi^b = 1/2 \phi'$

The result of stability analysis for the downstream slope gives  $F_s = 1,307$ .

###### • Stability analysis according to the total cohesion method

In order to calculating in the unsaturated area, the upstream, the impermeable core, and the downstream incremental loading masses above the saturate line are divided into thin layers (Figure 31).

The stability analysis result for the downstream slope of the earth dam using the total cohesion method gives the minimum stability factor according to Fredlund and Vanapalli equal 1,412 ( $F_s = 1,412$ ).

##### 4.2 Stability analysis of the khecat earth dam slope

###### 4.2.1 Seepage analysis

The analysis result of the pore water pressure using SEEP/W (GEOSTUDIO 2004) is shown in the Figure 32. From this, it is seen that the value of negative pore pressure in the area above the saturation line is under -200 kPa.

###### 4.2.2 Slope stability analysis

The slope stability analysis of Khecat earth dam is done by three methods: no consideration of  $\phi^b$ ; assumption  $\phi^b = 1/2 \phi'$ ; total cohesion.

###### • Slope stability analysis using no consideration of $\phi^b$ method

The result of stability analysis of the downstream slope for the earth dam according to this method gives the minimum stability factor equal  $F_s = 2,573$ .

###### • Slope stability analysis using assumption $\phi^b = 1/2 \phi'$

The result of stability analysis of the downstream slope for the earth dam according to this method gives the minimum stability factor equal  $F_s = 2,705$ .

###### • Slope stability analysis using total cohesion method

Figure 33 is the cross section for analyzing. The result of stability analysis of the downstream slope for the earth dam according to Fredlund and Vanapalli shows that  $F_s = 2,781$ .

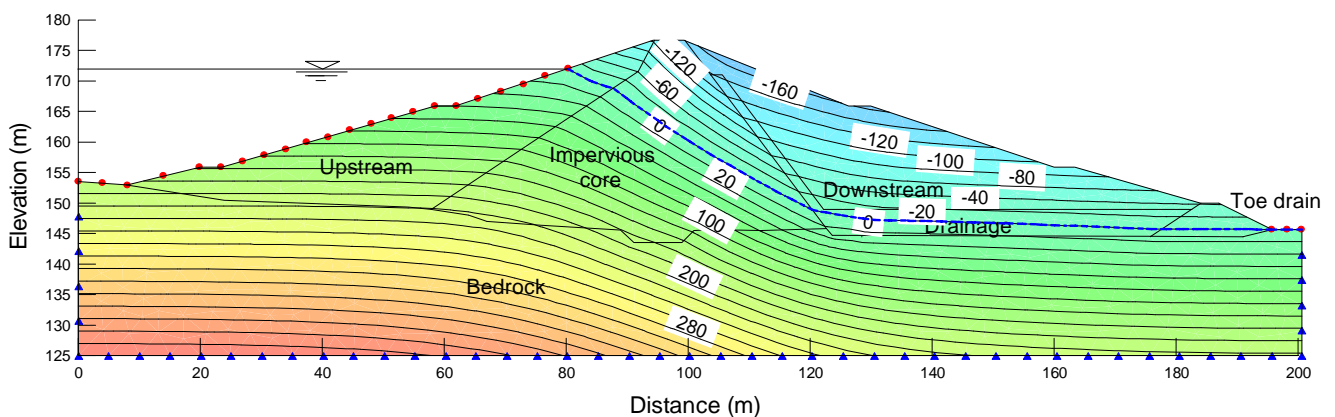


Figure 30 Pore pressure distribution lines in the dam body and foundation (MC5A)

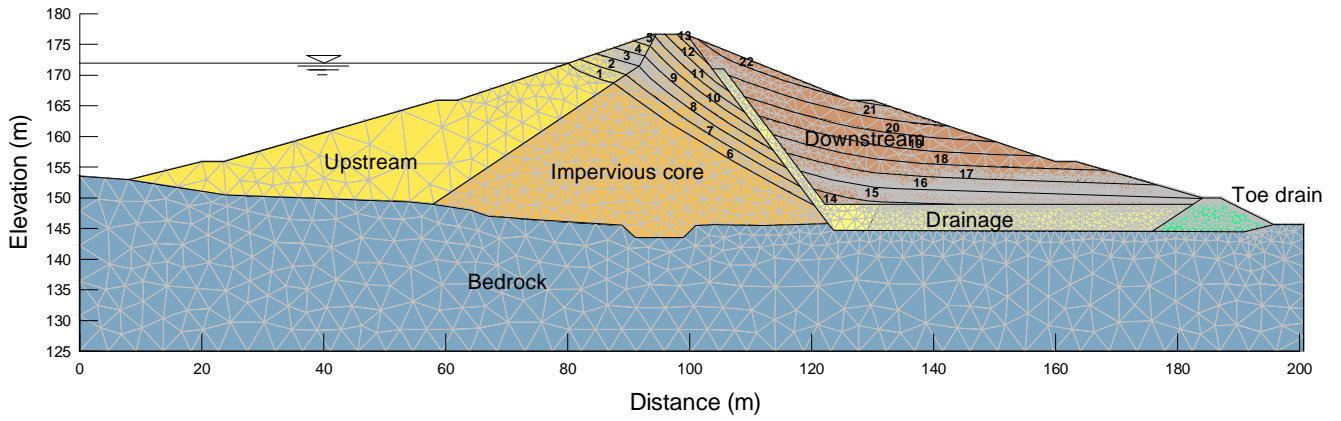


Figure 31 The stability analysis section according to total cohesion method

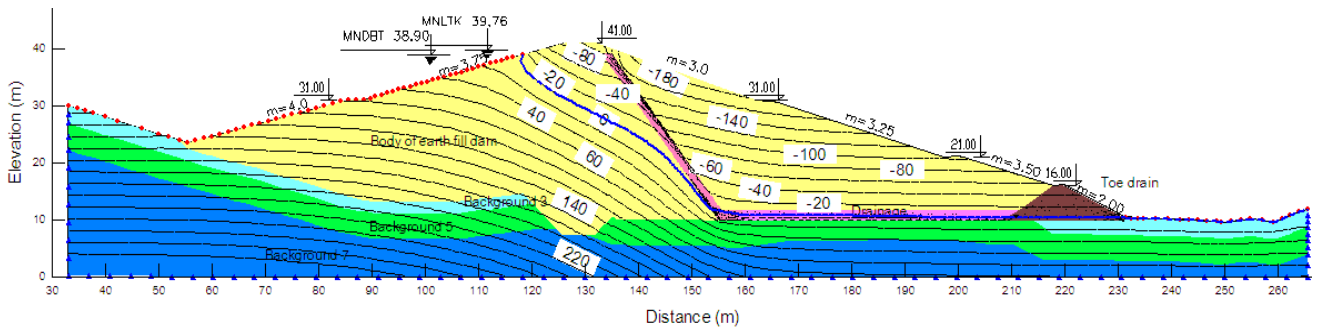


Figure 32 The water pore pressure distribution line in the dam body and its foundation (MC 0+200)

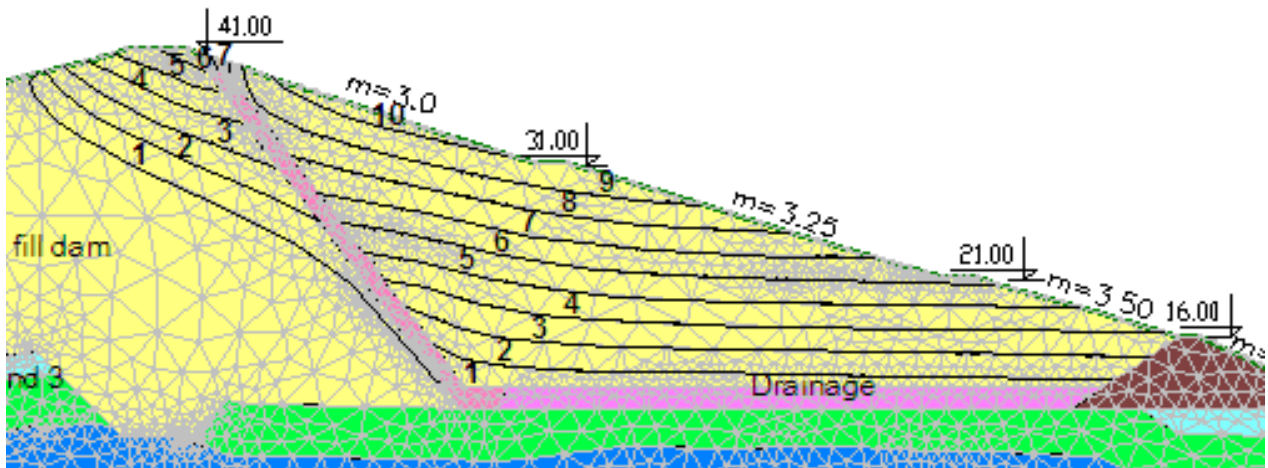


Figure 33 Cross section for analyzing stability according to total cohesion method

**4.3 Natural slope stability analysis in yenbai**

**4.3.1 Seepage analysis**

The results of pore water pressure analysis were estimated by using SEEP/W (GEOSTUDIO 2004). From this, it is seen that the negative pore pressure value in the soil area above the saturation line is inferior -180 kPa. The saturation line is founded on the measured data of actual underground level.

**4.3.2 Slope stability analysis**

Slope stability analysis is done by three methods: no consideration of  $\phi^b$ , assumption  $\phi^b = 1/2\phi'$  and total cohesion methods.

**• Stability analysis using no consideration of  $\phi^b$  method**

The result of slope stability analysis using this method gives the slope minimum stability coefficient equal  $F_s = 1,018$ .

**• Stability analysis using assumption  $\phi^b = 1/2\phi'$  method**

The calculated result for slope stability gives the minimum stability coefficient equal  $F_s = 1,250$ .

**• Stability analysis using total cohesion method**

The result of slope stability analysis using total cohesion slope method gives the minimum stability coefficient according to Fredlund and Vanapalli:  $F_s=1,258$ .

**4.4 Discussion of slope stability analysis results**

**4.4.1 The slope stability analysis results of Songsat dam**

The factor of safety of the earth fill dam slope by ignoring the unsaturated soil state, assuming  $\phi^b=1/2\phi'$  and using total cohesion method are shown in Figure 34. The factor of safety is 1,307 when assuming  $\phi^b=1/2\phi'$  and increases to 9,37% compared with ignoring unsaturated soil properties method (i.e.,  $F_s=1,195$ ). The factor of safety of slope gives the biggest value by using total cohesion method (i.e.,  $F_s=1,412$ ) and increases to 18,16% compared with ignoring unsaturated soil properties method.

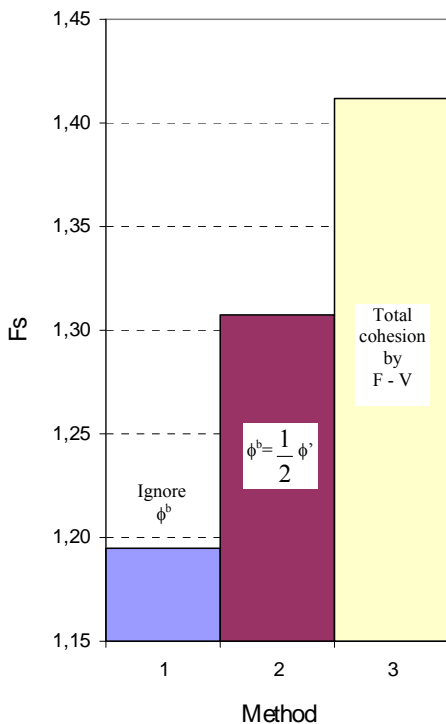


Figure 34 The slope stability analysis results of Songsat dam

**4.4.2 The slope stability analysis results of Khecat dam**

Figure 35 shows the factor of safety obtained from Khecat dam slope stability analysis by three methods. The factor of safety obtained when assuming  $\phi^b=1/2\phi'$  increase to 5,13% compared with ignoring unsaturated soil properties method while the one given by using total cohesion method increase to 8,08% (i.e.,  $F_s=2,781$ ).

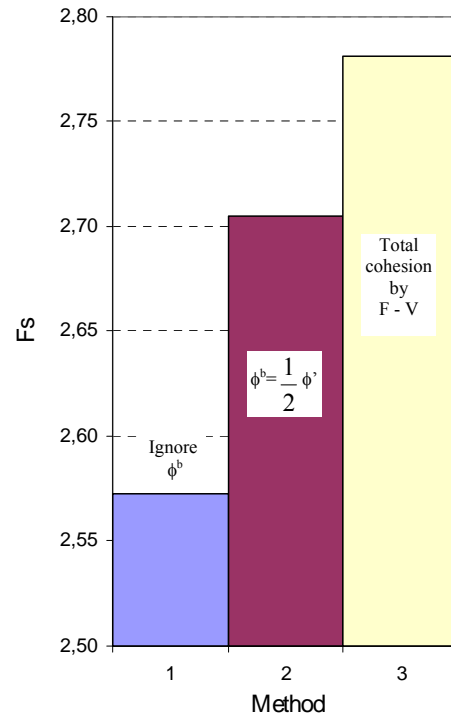


Figure 35 The slope stability analysis results of Khecat dam

The factor of safety obtained by using total cohesion method with the unsaturated soil properties suggested by Fredlund and Vanapalli gives the biggest value (i.e.,  $F_s=2,781$ ).

**4.4.3 The stability analysis results of natural slope in Yenbai**

The slope stability analysis results by three methods describe that the factor of safety obtained by assuming  $\phi^b=1/2\phi'$  method increases to 22,79% compared with ignoring unsaturated soil properties method while the one given by using total cohesion method increases to 23,58% (i.e.,  $F_s=1,258$ ).

**5. CONCLUSIONS**

This research has studied the theoretical basis about the saturated - unsaturated soil environment and the characteristic parameters of unsaturated soil. Analyzing and assessing the research and application situations of the characteristic parameters of unsaturated soil in the world, make clear the necessary of the study to find out and apply the unsaturated soil parameters in designing and constructing of structures in Vietnam.

The author has modified the normal triaxial apparatus at the Geotechnical Engineering lab of Water Resources University. In accordance with Fredlund and Rahardjo's model (1993) for researching. The part that was modified is the lower base of the triaxial cell and the air conductor pipe system on the top of the sample. This contribution shows that many labs in our country equipped with this type of apparatus can modify it in order to define unsaturated soils properties for many different targets and purposes.

The tests in order to find out unsaturated soil shear strength following different schemes gave the following results: when the soil sample turns from the saturated state to unsaturated state, the matric suction inside it increases, the internal friction angle  $\phi'$  is almost unchanged, however, its cohesive increases. The angle  $\phi^b = \phi'$  when the cohesive is smaller than the limit input air pressure value. Angle  $\phi^b$  started to decrease significantly at the cohesion values larger than the limit input air pressure value. The extended Mohr-Coulomb failure envelope surface for unsaturated soil samples is curved along the matric suction axis. The shear strength ( $\phi'$ ,  $c'$  and  $\phi^b$ ) of the same soil obtained by different cutting method (direct shear test, consolidation drain triaxial test, and shear with unchanged moisture content) gave approximately the same values, so the author suggests that in case lacking of laboratory triaxial apparatus for unsaturated soil, it is possible to use the direct shear one to find out the shear strength parameters of unsaturated soil followed the procedure as announced in the research.

Establishing the curves that can be used to calculate SWCC parameters, permeability coefficient and shear strength for some soil types in Vietnam helps people to avoid using unsuitable SWCC curves from other countries.

From testing to find out a set of characteristic parameters for some soil types in Vietnam as well as to show the influence of unsaturated characteristics on the stability of earth slopes in our country. The research results show that the unsaturated soil shear strength has a large influence on the stability state of earth dams. The less saturation for soil with higher matric suction, the permeability coefficient more reduces, the soil shear strength would increase, and it leads to increase the safety factor of the stability of the soil mass. This explains that the modified triaxial apparatus and direct shear test in the Vietnamese conditions are totally possible to find out the soil shear strength for earth dam design based on the calculation using saturated or unsaturated model.

Suggest a method to apply unsaturated soil parameters for earth slope stability analysis. This method satisfies the safety and economic conditions for Vietnamese soil. Earth dam design based on the slope stability calculation by the saturated or unsaturated models with the material parameters are defined based on laboratory tests on saturated/unsaturated soils allowing to reduce the slope's inclination so that the amount of fill material can be reduced without reducing the reliability. This is a base to improve the quality of the structures and to reduce the investment expenditure. This suggestion has a great meaning in expanding the area of selecting solutions for calculating and designing earthen structures, it also helps to design structures with suitable dimensions, safety and economy. Base on the character of Vietnamese climate, the author suggests some conditions to apply these calculated methods are: the construction area has not too high annual rainfall, the construction area is lack of local material, and the dam slope is designed not too steep to guarantee the safety for the dam when heavy rain occurs.

## 6. REFERENCES

- ASTM D 6838 - 02 - ASTM, (2003) Standard Test Method for Determination of the Soil Water Characteristic Curve for Desorption Using Hanging Column, Pressure Extractor, Chilled Mirror Hygrometer, and/or Centrifuge. Annual Book of ASTM Standards, Volume 04.08.
- Clifton, A.W., Wilson, G.W. and Barbour, S.L. (1999) "The Emergence of Unsaturated Soil Mechanics". Fredlund Volume, NRC Research Press, Ottawa, Ontario, Canada, 735 p.
- Fredlund, D.G. and Rahardjo, H. (1993) "Soil Mechanics for Unsaturated Soils". John Wiley and Sons Inc., New York.
- Fredlund, D.G. and Xing, A. (1994) Equations for the soil-water characteristic curve. Canadian Geotechnical Journal.
- Head, K.H. (1986) "Manual of Soil Laboratory Testing". John Wiley and Sons, Inc., Vol. 3, pp. 942-945.
- Hariato Rahardjo, Eng Choon Leong and Trinh Minh Thu (2005) "Application of soil-water characteristic curve in Geotechnical engineering". Proceedings of the international workshop, Hanoi geoengineering 2005, p.86 - 94.
- Hariato Rahardjo, (2006) "Rainfall-Induced Slope Failures". Short Course. Hanoi, Vietnam.
- Mancuso, C., Tarantino, A. (2005) "Unsaturated Soils. Advances in Testing, Modelling and Engineering Applications". Proceedings of the Second International Workshop on Unsaturated Soils, 23-25 June 2004, Anacapri, Italy, A.A. Balkema Publishers, a member of Taylor & Francis Group plc, London, UK.
- Ning Lu (Colorado School of Mines) and William J. Likos (University of Missouri-Columbia). (2004) "Unsaturated Soil Mechanics". John Wiley & Sons, Inc., Hoboken, New Jersey.
- TCVN 4195-1995 ÷ 4202-1995, (1996) Vietnam Standards: Engineering Soil. Ministry of Construction, Hanoi, Vietnam.
- Vanapalli, S.K. "A simple Experimental procedure for determining the fitting parameter,  $\kappa$  for predicting the shear strength of an unsaturated soil".